

General Regularities and Differences in the Behavior of the Dynamic Magnetization Switching of Ferrimagnetic (CoFe₂O₄) and Antiferromagnetic (NiO) Nanoparticles

S. I. Popkov^{a, b, *}, A. A. Krasikov^a, S. V. Semenov^{a, b}, A. A. Dubrovskii^a, S. S. Yakushkin^c,
V. L. Kirillov^c, O. N. Mart'yanov^c, and D. A. Balaev^{a, b}

^a Kirensky Institute of Physics, Krasnoyarsk Scientific Center, Siberian Branch, Russian Academy of Sciences, Krasnoyarsk, 660036 Russia

^b Siberian Federal University, Krasnoyarsk, 660041 Russia

^c Boreskov Institute of Catalysis, Siberian Branch, Russian Academy of Sciences, Novosibirsk, 630090 Russia

*e-mail: psi@ksc.krasn.ru

Received March 26, 2020; revised March 26, 2020; accepted April 2, 2020

Abstract—In antiferromagnetic (AFM) nanoparticles, an additional ferromagnetic phase forms and leads to the appearance in AFM nanoparticles of a noncompensated magnetic moment and the magnetic properties typical of common FM nanoparticles. In this work, to reveal the regularities and differences of the dynamic magnetization switching in FM and AFM nanoparticles, the typical representatives of such materials are studied: CoFe₂O₄ and NiO nanoparticles with average sizes 6 and 8 nm, respectively. The high fields of the irreversible behavior of the magnetizations of these samples determine the necessity of using strong pulsed fields (amplitude to 130 kOe) to eliminate the effect of the partial hysteresis loop when studying the dynamic magnetic hysteresis. For both types of the samples, coercive force H_C at the dynamic magnetization switching is markedly higher than H_C at quasi-static conditions. H_C increases as the pulse duration τ_p decreases and the maximum applied field H_0 increases. The dependence of H_C on field variation rate $dH/dt = H_0/2\tau_p$ is an unambiguous function for CoFe₂O₄ nanoparticles, and it is precisely such a behavior is expected from a system of single-domain FM nanoparticles. At the same time, for AFM NiO nanoparticles, the coercive force is no longer an unambiguous function of dH/dt , and the value of applied field H_0 influences more substantially. Such a difference in the behaviors of FM and AFM nanoparticles is caused by the interaction of the FM subsystem and the AFM “core” inside AFM nanoparticles. This circumstance should be taken into account when developing the theory of dynamic hysteresis of the AFM nanoparticles and also to take into account their practical application.

Keywords: CoFe₂O₄ nanoparticles, antiferromagnetic NiO nanoparticles, dynamic magnetization switching, coercive force

DOI: 10.1134/S1063783420090255

1. INTRODUCTION

Interest in magnetic nanoparticles is caused by an expansion of the area of their possible applying in practice and also by the fundamental problems related to the influence of surface and size effects on their magnetic characteristics. One of significant manifestations of surface and size effects is the formation of additional (besides the main) magnetic subsystems in nanoparticles. Here, first, we bear in mind the subsystem of surface spins [1–3] that can demonstrate the spin-glass behavior [3–5] and substantially modify spins in the particle “core” [6, 7]. Nanoparticles of antiferromagnetic (AFM) materials demonstrate a principally new property, namely, a noncompensated magnetic moment. It is assumed that a possible reason

of formation of a noncompensated moment in AFM nanoparticles is the existence of defects on the surface and also in the particle bulk [8, 9]. Actually, an additional ferromagnetic (FM) subsystem forms in a nanoparticle with AFM ordering [10–16].

The study of the dynamic magnetic hysteresis (DMH) is an advanced technique of studying the magnetic state in systems of nanoparticles [17–23]. This is caused by the necessity of understanding the influence of internal parameters of a material (magnetic anisotropy and particle size) on the shape of the DMH loop and also the applications in the hyperthermia. The dynamic hysteresis of single-domain FM particles is determined by relaxation processes of the particle magnetic moment [17, 18, 24, 25]. The existence of an FM subsystem in AFM nanoparticles

makes their behavior similar to the behavior of FM nanoparticles, and the dynamics of magnetization switching also influences the magnetic hysteresis loop form. DMH was considered theoretically in many works; in these cases, the dynamic magnetization switching are considered in FM nanoparticles [17, 18, 24–27] and also in AFM nanoparticles [28, 29]. The experimental works are limited by the studies of FM nanoparticles [3, 20–23, 30–32], and the attention is mainly focused on the hyperthermia effect, or more correctly, on its resulting characteristics, i.e., the heat release in the system under study placed in an ac field.

Common installations generating an ac magnetic field $H = H_0 \sin(2\pi\nu t)$ have substantial restrictions on the value of H_0 and frequency ν related to the power released in a solenoid. Thus, at frequencies 10^2 – 10^3 Hz, field H_0 is not higher than $\sim 10^3$ Oe [21, 32]. This circumstance substantially hampers studying DMH in materials which are characterized by high magnetic anisotropy, since the resulting hysteresis loop will be partial if H_0 is lower than the field of irreversible behavior of magnetization H_{irr} .

An alternative to the standard methods of studying DMH is the use of pulsed field at which the power release is limited by one cycle of varying the external field, and there is a possibility to increase field H_0 up to several hundreds kOe. Then, at $H_0 > H_{\text{irr}}$, the obtained coercive force H_C already will characterize a close hysteresis loop and will be determined by the material magnetic anisotropy, particle sizes and pulse parameters [33, 34].

This work is devoted to a comparative study of typical representative ferrimagnetic (CoFe_2O_4 ; in what follow, these materials will be noted FM) and AFM (NiO) nanoparticles, for which condition $H_0 > H_{\text{irr}}$ can be achieved only using pulsed fields. The main aim of this work is to show which of external parameters are determining for the coercive force of such various systems under the conditions of dynamic magnetization switching.

2. EXPERIMENTAL

We studied samples of NiO and CoFe_2O_4 nanoparticles with average sizes 8 and 6 nm, respectively. The preparation technique and the characterization including X-ray diffraction and transmission electron microscopy are described in [35, 36]. The quasi-static magnetic properties were measured using a vibrating-sample magnetometer (VSM). Temperature dependences of the magnetization $M(T)$ were measured on cooling in a zero external field (ZFC) and on cooling in a field (FC). Field dependences of the magnetization $M(H)$ were measured in ZFC conditions. The quasi-static hysteresis loops $M(H)$ were measured at the field variation rate $(dH/dt)_{\text{VSM}}$ of ~ 50 Oe/s. To obtain the dependence of H_C on the maximum applied

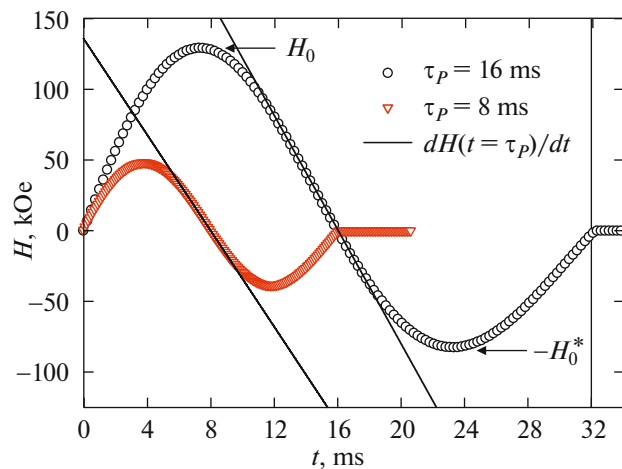


Fig. 1. Typical time dependences of the solenoid field obtained by the pulsed technique at various values of H_0 and τ_p . The slopes of the straight lines correspond to the field variation rate dH/dt in the vicinity of $H = 0$.

field H_0 , we measured a family of partial hysteresis loops as the value H_0 sequentially increased.

Dependences $M(H)$ under conditions of dynamic magnetization switching were studied on an original installation at the Kirensky Institute of Physics of Siberian Branch, Russian Academy of Sciences, in which the standard method of discharging the capacitor bank through a solenoid [37] is used. To form two half-waves, diodes were included counter-parallel to a thyristor in the installation circuit. Figure 1 shows the typical dependences of the field in the solenoid on time at various H_0 (the values H_0 are determined by the capacitor charge voltage) and on the pulse duration (half-wave duration) τ_p . The value of τ_p was varied by a commutation of the capacitor bank blocks for various capacities. The measurements were carried out at τ_p of 8 and 16 ms. A zero value of the field at moment $t = 2\tau_p$ is due to closing the blocks of thyristors. The rate of varying the magnetic field dH/dt in the vicinity of $H = 0$ was determined as the slopes of the tangents to dependences $H(t)$ as shown in Fig. 1.

The magnetization was measured using an induction pickup that was a system of coaxial compensated coils, to which a sample was placed. The signal induced in the coils was amplified and recorded by a digital storage oscilloscope. At the same temperature, the value of H_0 in each subsequent measurement was higher than that in the preceded measurement.

3. RESULTS AND DISCUSSION

3.1. Temperature Dependence of the Magnetization $M(T)$

Figure 2 shows the temperature dependences of the magnetization $M(T)$ of the samples studied in ZFC

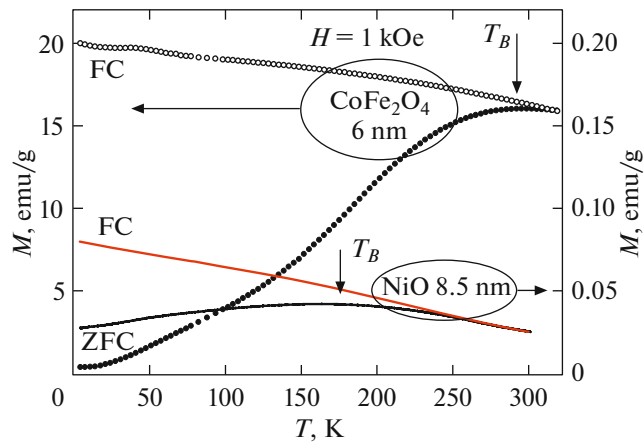


Fig. 2. Temperature dependences $M(T)$ for the samples under study measured in the ZFC and FC (in field $H = 1$ kOe) conditions.

and FC conditions in field $H = 1$ kOe. From these dependences, it can be concluded that the samples demonstrate the behavior characteristic of the blocked state (at low temperatures) and the unlocked (supermagnetic (SPM)) state at high temperatures. Dependences $M(T)_{ZFC}$ have clear maxima, in the vicinity of which dependences $M(T)_{ZFC}$ and $M(T)_{FC}$ diverge. According to our data, the maxima in dependences $M(T)_{ZFC}$ shift to lower temperatures as the external field increases. Temperatures T_B in the maximum point (as a first approximation, the temperature of the SPM blocking) of dependences $M(T)_{ZFC}$ are ~ 290 K and ~ 160 K for the CoFe_2O_4 and NiO samples, respectively. These values agree well with the data for the SPM blocking obtained for CoFe_2O_4 nanoparti-

cles [38, 39] and NiO nanoparticles [39, 40] of similar sizes.

3.2. Magnetic Hysteresis in Quasi-Stationary Conditions

Figure 3 shows dependences $M(H)$ of the samples at $T = 80$ K obtained as a family of partial loops with sequentially increasing values of H_0 to 60–70 kOe. It is seen that the loop for CoFe_2O_4 nanoparticles (Fig. 3a) becomes closed at $H_0 \approx 30$ kOe, and the further increase in H_0 does not lead to a change in the hysteresis loop form (the inset in Fig. 3a). For NiO (Fig. 3b) at $H_0 \approx 50$ –70 kOe, dependence $M(H)$ is still irreversible at high fields, although, in the vicinity of the origin of coordinates, the loops obtained at quite high values of H_0 are already close to each other (the inset in Fig. 3b). Note that the form of dependence $M(H)$ for NiO is typical of AFM nanoparticles [10, 11, 16, 41–44] and reflects the existence of several magnetic subsystems (within one particle). The hysteresis behavior is determined by the FM subsystem, and the marked linear increase in $M(H)$ is determined by the AFM susceptibility of the particle “core” and other contributions [43, 44].

3.3. Magnetic Hysteresis in Pulsed Fields

Figure 4 shows typical dependences $M(H)$ obtained by the VSM method and by the pulsed magnetometer method (at $T = 80$ K). Dependences $M(H)$ for CoFe_2O_4 (Fig. 4a) clearly demonstrate the saturation in fields of 60–80 kOe. The value of the field of irreversible behavior of magnetization H_{irr} is very weakly dependent on the technique of measurements ($H_{\text{irr}} \approx 30$ kOe). For NiO (Fig. 4b), the irreversibility of

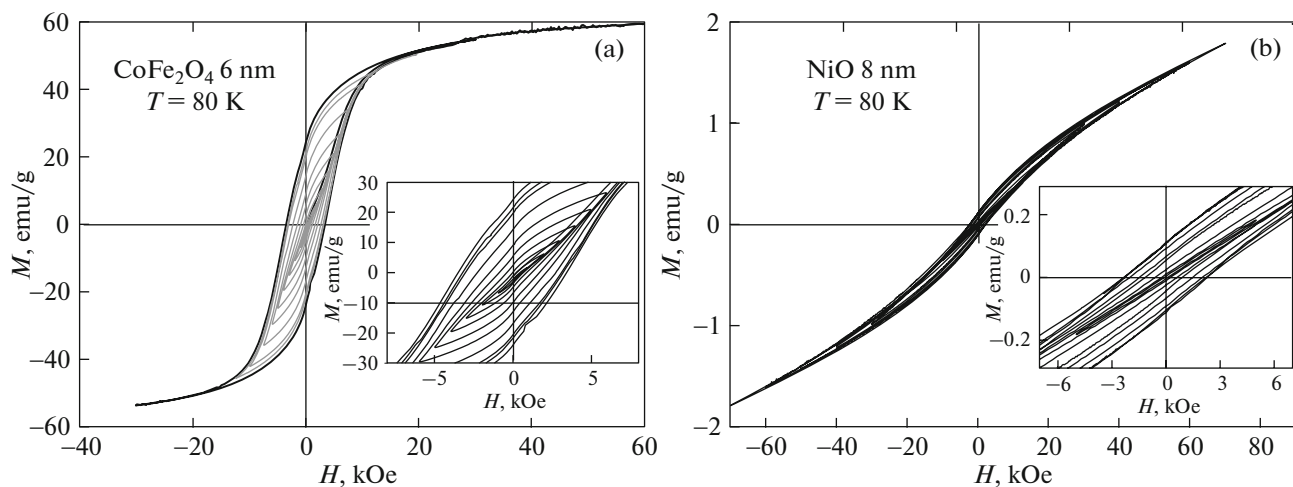


Fig. 3. Magnetic hysteresis loops at $T = 80$ K for (a) 6-nm CoFe_2O_4 and (b) 8-nm NiO nanoparticles measured by the VSM technique at a sequential increase in the maximum applied field. The insets show the portions of partial loops in the vicinity of the origin of coordinates.

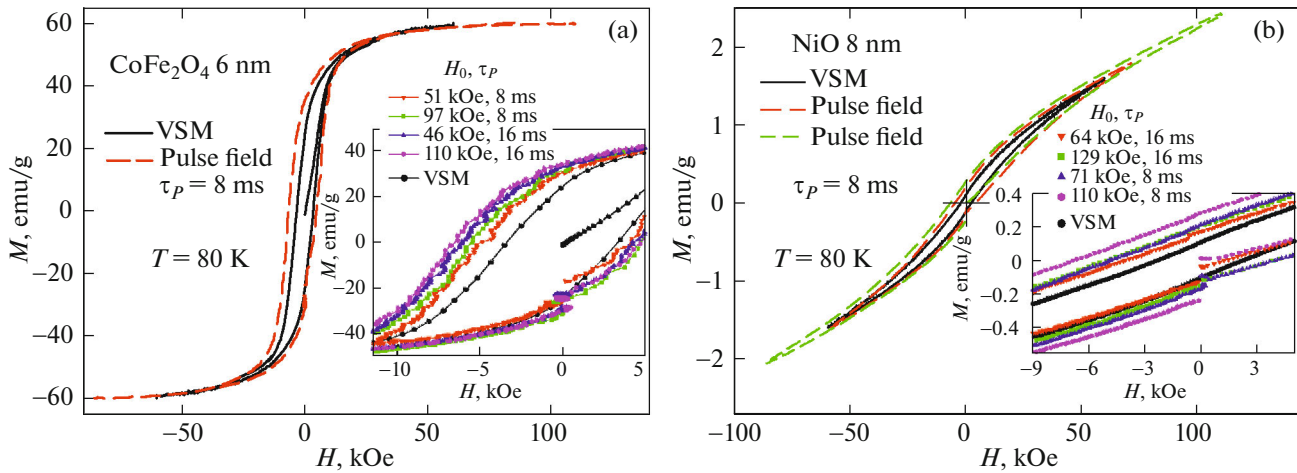


Fig. 4. Hysteresis loops at $T = 80$ K for (a) CoFe_2O_4 and (b) NiO nanoparticles measured by the VSM technique and in pulsed fields at various pulse parameters (the values of τ_p and H_0 are given in Figs. 4a and 4b). The insets show dependences $M(H)$ in the vicinity of the origin of coordinates.

dependence $M(H)$ at high fields in the case of the pulsed technique becomes more noticeably than that for the VSM data (Fig. 3b). At the measurements in a pulsed field (Fig. 1), only hysteresis loop parts are recorded in the field ranges: (i) $0-H_0$, (ii) $H_0-(-H_0^*)$, and (iii) $(-H_0^*)-0$, where $|H_0^*| < H_0$ (Fig. 1). Region (ii) is the most informative part for the pulsed technique, and, it is seen from Fig. 4 that the hysteresis loops are markedly widened in region (ii). In addition, from the data shown in Fig. 4 and in the insets to it, it is seen that the decrease in τ_p and the increase in H_0 lead to the increase in H_C for the samples of both types. Therefore, the general regularity for FM and AFM nanoparticles at the dynamic magnetization switching is an increase in H_C with H_0 and τ_p , while, for NiO nanoparticles, the loops remain open up to fields higher than 100 kOe.

3.4. The Dependence of H_C on the Pulse Parameters

In our experiments with a pulsed field, H_0 almost always is significantly higher than H_C , and, in the vicinity of $H \sim H_C$, the field variation rate $dH/dt \approx \text{const}$ (Fig. 1). The approximation of dependence $H(t)$ by harmonic law $H(t) \approx H_0 \sin(t/2\tau_p)$ gives $t \sim \tau_p$

$$(dH/dt)_{(t=\tau_p)} = H_0/2\tau_p.$$

Therefore, dH/dt is determined by the ratio of the parameters (H_0 and τ_p) varied during the measurements in a pulsed field.

To reveal the regularities and differences in the behavior of DMH for AFM and FM nanoparticles, we focus our attention on the influence of H_0 and dH/dt on H_C . Figure 5 illustrates dependences $H_C(H_0)$ (Fig. 5c) and $H_C(dH/dt)$ (Figs. 5b, 5d) for the

CoFe_2O_4 (Figs. 5a, 5b) and NiO (Figs. 5c, 5d) samples. Note that the character of the dependences shown in Fig. 5 is typical of the temperature range 80–250 K. The increase in H_C with H_0 is clearly seen in Figs. 5a, 5c. At a certain temperature, the experimental points for CoFe_2O_4 at various τ_p (Fig. 5a) are separated into two quite distant dependences. On the other hand, in the H_C-dH/dt coordinates, the points for CoFe_2O_4 in Fig. 5b are clearly lie on the same functional dependence (at $T = \text{const}$). And this fact is logic, since it is parameter dH/dt that is basic in the dynamic magnetization switching processes [33, 34].

For NiO (Figs. 5c, 5d), we see another situation. In the H_C-H_0 coordinates, the data for $\tau_p = 8$ and 16 ms correspond to two different dependences (Fig. 5c); however, these groups of the points are disposed much closer to one other, than in the case of CoFe_2O_4 (Fig. 5a). On the other hand, in the H_C-dH/dt coordinates (Fig. 5c), the data for NiO do not lie on the same functional dependence (as in the case of CoFe_2O_4 , Fig. 5b) and, conversely, they are separated in two dependences distant from one another and corresponding to various values of τ_p . Therefore, there is no longer unambiguous dependence of H_C on dH/dt for AFM NiO nanoparticles. Similar behavior was observed during the pulsed magnetization switching of AFM nanoparticles of ferrihydrite [45].

Consider possible reasons of this difference. For CoFe_2O_4 nanoparticles at $T = 80$ K, dependences $M(H)$ demonstrate the saturation in fields higher than ~ 60 kOe (Fig. 4a); in this case, in fields higher than $H_{\text{irr}} \approx 30$ kOe, dependence $M(H)$ is completely reversible, the hysteresis loop is closed, but the value of H_{irr} is only slightly changed under conditions of the pulsed magnetization switching. This result completely corre-

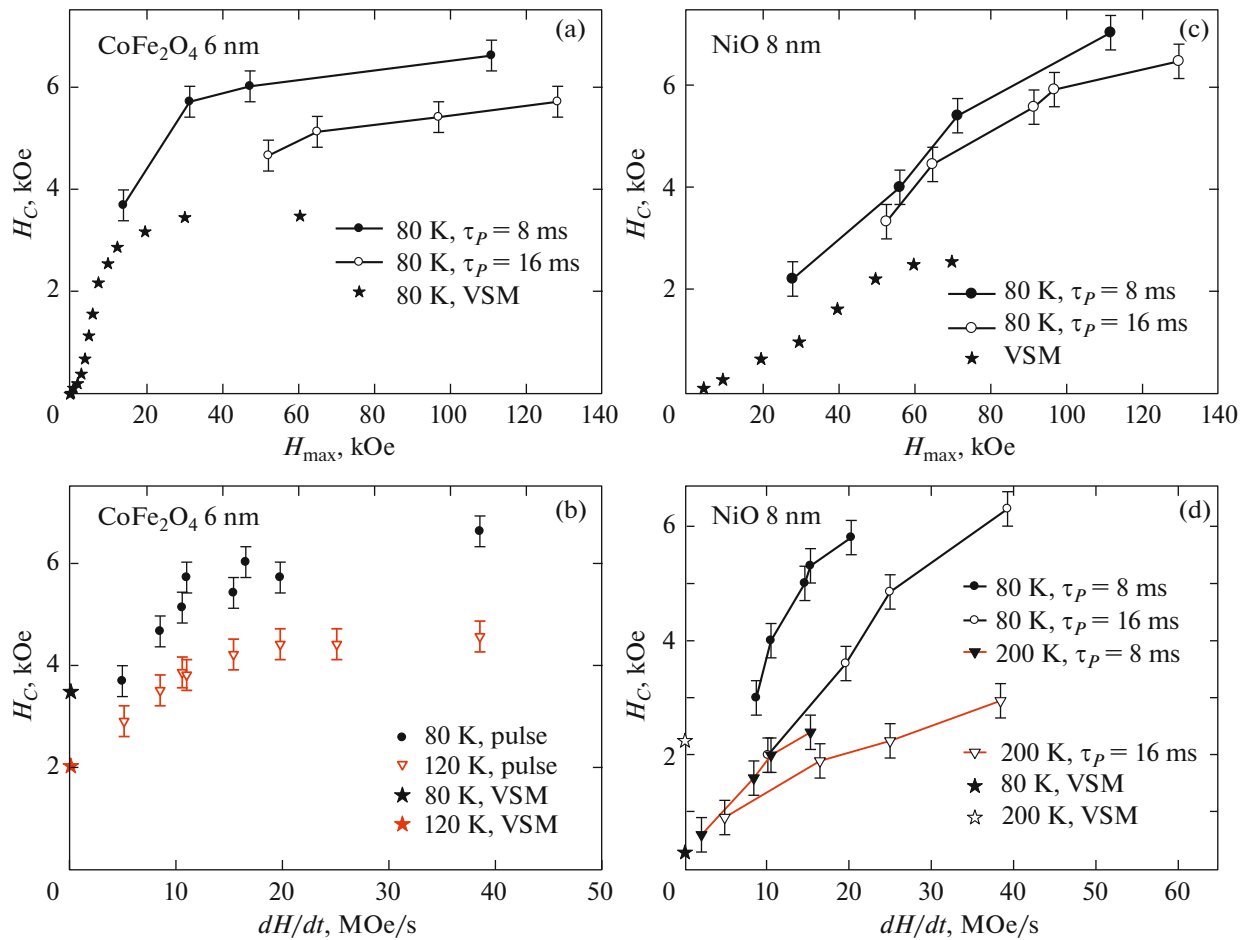


Fig. 5. Behavior of coercive force H_C at pulsed magnetization switching as a function of parameters (a, c) H_0 and (b, d) dH/dt for (a, b) 6-nm CoFe_2O_4 and (c, d) 8-nm NiO nanoparticles measured at the noted parameters; the VSM data are shown, too. In panels (a, c, d), the data are grouped by the pulse durations by connecting lines.

sponds to the standard description of the behavior of single-domain FM particles, for which the magnetic hysteresis is determined by the competition of the Zeeman energy and the magnetic anisotropy energy. The magnetic hysteresis for the AFM nanoparticles can be described, in principle, using similar approach with the reserve that, in this case, the FM subsystem of an AFM nanoparticle “operates.”

The AFM nanoparticles are known to be characterized by high values of fields H_{irr} , and we usually observe the S -shaped dependence $H_C(H_0)$ that tends to the saturation at high H_0 [16, 42, 46]. The VSM data in Fig. 5c confirm this fact: dependence $H_C(H_0)$ is almost “flattened” (at $H_0 \approx 70$ kOe), similar to the VSM results for CoFe_2O_4 (Fig. 5a). However, the hysteresis loops for NiO nanoparticles remain open up to high values of H_0 (Fig. 3b), and, in pulsed fields, the difference between the magnetizations in the increased and decreased fields becomes much more (Fig. 4b).

The foregoing indicates an additional contribution that influences the magnetization switching of the FM subsystem in AFM nanoparticles. This contribution is related to the interaction of magnetic subsystems in an AFM nanoparticle. There are many experimental facts demonstrating the interaction of the subsystem of surface spins with an AFM “core” nanoparticles, which are accompanied by the effects, such as the exchange shift of the hysteresis loop [14, 15, 42, 46] and spin-glass behavior of surface spins [4–7, 40, 41]. However, these effects are mainly observed at low temperatures that are much lower than the SPM blocking temperatures. The behavior of DMH of NiO nanoparticles discussed in this work is characteristic not only at $T = 80$ K, but also at $T > T_B$ (Fig. 5d). Therefore, the relationship of the FM subsystem already with an AFM “core” can be the cause of the observed difference in the behavior of DMH for the FM and AFM nanoparticles. In the “dynamic” conditions, i.e., in the conditions of the pulsed magnetization switching, the rela-

tionship of the FM subsystem with an AFM “core” must be observed more clearly.

4. CONCLUSIONS

We performed the comparative study of the dynamic magnetization switching in pulsed fields with a strength up to 130 kOe of nanoparticles of the CoFe_2O_4 ferrimagnet (6 nm) and NiO antiferromagnet (8 nm). The use of the pulsed field technique is caused by high values of the irreversible behavior of the magnetization of the objects noted above. Both types of the nanoparticles demonstrate the transition from the blocked (the existence of the hysteresis loop) to the unblocked state at the SPM-blocking temperatures ~ 290 K and ~ 160 K for the CoFe_2O_4 and NiO samples, respectively. At the pulsed magnetization switching, coercive force H_C is higher than that in the quasi-static conditions, and H_C increases for the nanoparticles of both the types as pulse duration τ_p decreases and the maximum field H_0 increases. Such a behavior is related to the relaxation processes typical of single-domain FM particles, but, in the case of AFM NiO nanoparticles, we should speak about the FM subsystem, i.e., the noncompensated magnetic moment of an AFM nanoparticle. For FM nanoparticles, the field variation rate $dH/dt = H_0/2\tau_p$ is a parameter that unambiguously determines the value H_C at the pulsed magnetization switching. However, the AFM nanoparticles demonstrate more complex behavior: there is no unambiguous dependence of H_C on dH/dt and the value H_0 plays a larger role than for FM nanoparticles. This fact can be considered as a feature characteristic of the class of AFM nanoparticles that should be taken into account when developing the theory of DMH of AFM nanoparticles and also during their possible application in heat release processes upon the magnetization switching (for example, at hyperthermia). The mechanism leading to the noted difference in the behavior of DMH of the AFM and FM nanoparticles is related to the interaction of magnetic subsystems in an AFM nanoparticle, i.e., the magnetic binding” of the FM subsystem (noncompensated moment) and the AFM “core.”

FUNDING

This work was supported by the Russian Foundation for Basic Research, the Government of the Krasnoyarsk region, and the Krasnoyarsk Regional Foundation for Science, project no. 18-42-240012: “Magnetization switching of magnetic nanoparticles in strong pulsed magnetic fields is a new approach to studying the dynamic effects related to the processes of magnetization of magnetic nanoparticles.”

CONFLICT OF INTEREST

The authors declare that they have no conflicts of interest.

REFERENCES

1. K. Nadeem, H. Krenn, T. Traussnig, R. Würschum, D. V. Szabo, and I. Letofsky-Papst, *J. Appl. Phys.* **111**, 113911 (2012).
2. S. S. Yakushkin, A. A. Dubrovskiy, D. A. Balaev, K. A. Shaykhutdinov, G. A. Bukhtiyarova, and O. N. Martyanov, *J. Appl. Phys.* **111**, 044312 (2012).
3. A. S. Kamzin, A. A. Valiullin, V. G. Semenov, H. Das, and N. Wakiya, *Phys. Solid State* **61**, 1113 (2019).
4. M. Tadic, D. Nikolic, M. Panjan, and G. R. Blake, *J. Alloys Compd.* **647**, 1061 (2015).
5. S. V. Stolyar, D. A. Balaev, V. P. Ladygina, A. I. Pankrats, R. N. Yaroslavtsev, D. A. Velikanov, and R. S. Iskhakov, *JETP Lett.* **111**, 183 (2020).
6. R. H. Kodama and A. E. Berkowitz, *Phys. Rev. B* **59**, 6321 (1999).
7. A. P. Safronov, I. V. Beketov, S. V. Komogortsev, G. V. Kuryandskaya, A. I. Medvedev, D. V. Leiman, A. Larranaga, and S. M. Bhagat, *AIP Adv.* **3**, 052135 (2013).
8. L. Neel, *C. R. Acad. Sci. Paris* **252**, 4075 (1961).
9. Yu. L. Raikher and V. I. Stepanov, *J. Exp. Theor. Phys.* **107**, 435 (2008).
10. A. A. Lepeshev, I. V. Karpov, A. V. Ushakov, D. A. Balaev, A. A. Krasikov, A. A. Dubrovskiy, D. A. Velikanov, and M. I. Petrov, *J. Supercond. Nov. Magn.* **30**, 931 (2017).
11. S. A. Makhlof, F. T. Parker, F. E. Spada, and A. E. Berkowitz, *J. Appl. Phys.* **81**, 5561 (1997).
12. S. I. Popkov, A. A. Krasikov, A. A. Dubrovskiy, M. N. Volochaev, V. L. Kirillov, O. N. Martyanov, and D. A. Balaev, *J. Appl. Phys.* **126**, 103904 (2019).
13. D. A. Balaev, A. A. Dubrovskiy, A. A. Krasikov, S. I. Popkov, A. D. Balaev, K. A. Shaikhutdinov, V. L. Kirillov, and O. N. Mart’yanov, *Phys. Solid State* **59**, 1547 (2017).
14. S. A. Makhlof, H. Al-Attar, and R. H. Kodama, *Solid State Commun.* **145**, 1 (2008).
15. M. S. Seehra and A. Punnoose, *Solid State Commun.* **128**, 299 (2003).
16. D. A. Balaev, A. A. Krasikov, S. V. Stolyar, R. S. Iskhakov, V. P. Ladygina, R. N. Yaroslavtsev, O. A. Bayukov, A. M. Vorotynov, M. N. Volochaev, and A. A. Dubrovskiy, *Phys. Solid State* **58**, 1782 (2016).
17. I. S. Poperechny, Yu. L. Raikher, and V. I. Stepanov, *Phys. Rev. B* **82**, 174423 (2010).
18. S. Poperechny and Yu. L. Raikher, *Phys. B (Amsterdam, Neth.)* **435**, 58 (2014).
19. Y. P. Kalmykov, S. V. Titov, W. T. Coffey, M. Zarifakis, and W. J. Dowlin, *Phys. Rev. B* **99**, 184414 (2019).
20. E. L. Verde, G. T. Landi, J. A. Gomes, M. H. Sousa, and A. F. Bakuzis, *J. Appl. Phys.* **111**, 123902 (2012).
21. Y. Lv, Y. Yang, J. Fang, H. Zhang, E. Peng, X. Liu, W. Xiao, and J. Ding, *RSC Adv.* **5**, 76764 (2015).
22. E. Garaio, O. Sandre, J.-M. Collantes, J. A. Garcia, S. Mornet, and F. Plazaola, *Nanotechnology* **26**, 015704 (2015).
23. A. S. Kazmin, I. M. Obaidat, A. A. Valliulin, V. G. Semenov, I. A. Al-Omari, and C. Nayek, *Tech. Phys. Lett.* **45**, 426 (2019).

24. N. A. Usov and Yu. B. Grebenshchikov, *J. Appl. Phys.* **106**, 023917 (2009).
25. J. Carrey, B. Mehdaoui, and M. Respaud, *J. Appl. Phys.* **109**, 083921 (2011).
26. A. M. Shutyi and D. I. Sementsov, *Phys. Solid State* **61**, 1736 (2019).
27. A. M. Shutyi and D. I. Sementsov, *J. Exp. Theor. Phys.* **129**, 248 (2019).
28. B. Ouari, S. Aktaou, and Y. P. Kalmykov, *Phys. Rev. B* **81**, 024412 (2010).
29. B. Ouari and Y. P. Kalmykov, *Phys. Rev. B* **83**, 064406 (2011).
30. A. S. Kamzin, A. A. Valiullin, H. Khurshid, Z. Nemati, H. Srikanth, and M. H. Phan, *Phys. Solid State* **60**, 382 (2018).
31. A. S. Kamzin, D. S. Nikam, and S. H. Pawar, *Phys. Solid State* **59**, 156 (2017).
32. C. Caizer and I. Hrianca, *Eur. Phys. J. B* **31**, 391 (2003).
33. D. A. Balaev, I. S. Poperechny, A. A. Krasikov, K. A. Shaikhutdinov, A. A. Dubrovskiy, S. I. Popkov, A. D. Balaev, S. S. Yakushkin, G. A. Bukhtiyarova, O. N. Mart'yanov, and Yu. L. Raikher, *J. Appl. Phys.* **117**, 063908 (2015).
34. S. I. Popkov, A. A. Krasikov, S. V. Semenov, A. A. Dubrovskii, S. S. Yakushkin, V. L. Kirillov, O. N. Mart'yanov, and D. A. Balaev, *Phys. Solid State* **62**, 445 (2020).
35. D. A. Balaev, A. A. Krasikov, A. A. Dubrovskii, A. D. Balaev, S. I. Popkov, V. L. Kirillov, and O. N. Mart'yanov, *J. Supercond. Nov. Magn.* **32**, 405 (2019).
36. D. A. Balaev, S. V. Semenov, A. A. Dubrovskii, A. A. Krasikov, S. I. Popkov, S. S. Yakushkin, V. L. Kirillov, and O. N. Mart'yanov, *Phys. Solid State* **62**, 285 (2020).
37. A. A. Bykov, S. I. Popkov, A. M. Parshin, and A. A. Krasikov, *J. Surf. Invest.: X-ray, Synchrotr. Neutron Tech.* **9**, 111 (2015).
38. G. Baldi, D. Bonacchi, C. Innocenti, G. Lorenzi, and C. Sangregorio, *J. Magn. Magn. Mater.* **311**, 10 (2007).
39. A. McDannald, M. Staruch, and M. Jai, *J. Appl. Phys.* **112**, 123916 (2012).
40. S. Baran, A. Hoser, B. Penc, and A. Szytula, *Acta Polon. A* **129**, 35 (2016).
41. N. Rinaldi-Montes, P. Gorria, D. Martínez-Blanco, A. B. Fuertes, L. Fernández Barquín, I. Puente-Orench, and J. A. Blanco, *Nanotechnology* **26**, 305705 (2015).
42. N. J. O. Silva, V. S. Amaral, A. Urtizberea, R. Bustamante, A. Millán, F. Palacio, E. Kampert, U. Zeitler, S. de Brion, O. Iglesias, and A. Labarta, *Phys. Rev. B* **84**, 104427 (2011).
43. N. J. O. Silva, A. Millan, F. Palacio, E. Kampert, U. Zeitler, and V. S. Amaral, *Phys. Rev. B* **79**, 104405 (2009).
44. S. I. Popkov, A. A. Krasikov, D. A. Velikanov, V. L. Kirillov, O. N. Mart'yanov, and D. A. Balaev, *J. Magn. Magn. Mater.* **483**, 21 (2019).
45. D. A. Balaev, A. A. Krasikov, D. A. Velikanov, S. I. Popkov, N. V. Dubynin, S. V. Stolyar, V. P. Ladygina, and R. N. Yaroslavtsev, *Phys. Solid State* **60**, 1973 (2018).
46. D. A. Balaev, A. A. Krasikov, A. A. Dubrovskiy, S. I. Popkov, S. V. Stolyar, R. S. Iskhakov, V. P. Ladygina, and R. N. Yaroslavtsev, *J. Appl. Phys.* **120**, 183903 (2016).

Translated by Yu. Ryzhkov